

# Land-atmosphere interactions in an high resolution atmospheric simulation coupled with a surface data assimilation scheme

L. Campo<sup>1</sup>, F. Castelli<sup>1</sup>, D. Entekhabi<sup>2</sup>, and F. Caparrini<sup>3</sup>

<sup>1</sup>Dipartimento di Ingegneria Civile e Ambientale, Università degli Studi di Firenze, Via S. Marta 3, 50139 Firenze, Italy

<sup>2</sup>Parsons Laboratory, Massachusetts Institute of Technology, Cambridge, MA 02139, USA

<sup>3</sup>Eumechanos – Via La Marmora 22, 50121 Firenze, Italy

Received: 14 April 2009 – Revised: 3 August 2009 – Accepted: 6 September 2009 – Published: 30 September 2009

**Abstract.** A valid tool for the retrieving of the turbulent fluxes that characterize the surface energy budget is constituted by the remote sensing of land surface states. In this study sequences of satellite-derived observations (from SEVIRI sensors aboard the Meteosat Second Generation) of Land Surface Temperature have been used as input in a data assimilation scheme in order to retrieve parameters that describe energy balance at the ground surface in the Tuscany region, in central Italy, during summer 2005. A parsimonious 1-D multiscale variational assimilation procedure has been followed, that requires also near surface meteorological observations. A simplified model of the surface energy balance that includes such assimilation scheme has been coupled with the limited area atmospheric model RAMS, in order to improve in the latter the accuracy of the energy budget at the surface. The coupling has been realized replacing the assimilation scheme products, in terms of surface turbulent fluxes and temperature and humidity states during the meteorological simulation. Comparisons between meteorological model results with and without coupling with the assimilation scheme are discussed, both in terms of reconstruction of surface variables and of vertical characterization of the lower atmosphere. In particular, the effects of the coupling on the moisture feedback between surface and atmosphere are considered and estimates of the precipitation recycling ratio are provided. The results of the coupling experiment showed improvements in the reconstruction of the surface states by the atmospheric model and considerable influence on the atmospheric dynamics.

## 1 Introduction

The estimation of the turbulent heat exchanges at the surface is of great importance in most hydrological and meteorological applications. A correct description of such phenomena can considerably improve the performances in numerical models in terms, respectively, of a more accurate hydrologic balance at watershed scale and of correct surface forcing for the atmospheric boundary layer. A significant influence is also observed on the precipitation: the evapotranspiration flux affects rain through a feedback mechanism that involves the soil moisture state (Entekhabi et al., 1996).

In the atmospheric numerical models, due to scale resolving limitations, parametrization of these surface processes is often present. For example, soil moisture storage and transfer processes in GCM (Global Circulation Models) are often oversimplified. Redistribution due to topography and numerous other important processes that may significantly contribute to land-atmosphere interaction are neglected (Entekhabi, 1995). On the other side, the growing attention on this topic produced in the last decade more accurate representations of the surface processes in the atmospheric numerical models, both LAM (Limited Area Models) and GCM (Vidale and Stöckli, 2005; Beljaars et al., 2007). In order to improve the performances of the atmospheric simulation at the surface, other approaches proposed couplings between atmospheric and surface models (Koster and Suarez, 1993; Dudhia and Chen, 1999; Haggag et al., 2008).

The direct measure of the turbulent fluxes presents several difficulties, due to the costs of installation and maintaining of the towers instruments (Baldocchi, 2001). This is particularly true at temporal and spatial resolutions that are significant for the study of two-way land-atmosphere interactions such as soil moisture feedback on precipitation (Entekhabi and Eagleson, 1989). A valid and largely utilized alterna-



Correspondence to: L. Campo  
(lcampo1@dicea.unifi.it)

tive to point surface measures for these variables is constituted by remote sensing. Measurements from satellite sensors are not directly related to heat and moisture fluxes, but they can be merged with models to infer physical conditions at the land surface that are intimately related to the energy balance. Among these conditions the Land Surface Temperature (LST) is the main prognostic variable for the indirect estimation of surface energy fluxes (Schulz et al., 1998).

A feasible general methodology to estimate surface energy fluxes based on remote observations is constituted by the combined use of LST and micrometeorological measurements in order to estimate the contribution of each flux component to the total surface energy balance. A possible approach consists in using data assimilation techniques of remote observations of surface radiometric temperature in order to solve the energy balance (Caparrini, 2001; Harris and Taylor, 2007; Meng et al., 2009). The first proposal of use of LST retrieved from satellite observations came from Wetzel et al. (1984), while a number of work have been proposed in last two decades about land data assimilation inside atmospheric models (McNider et al., 1994; Jones et al., 1998a, b; Giard and Bazile, 2000; Mahfouf et al., 2000; Van den Hurk and The, 2002; Bélair et al., 2003a, b).

In this study a variational approach has been followed using sequences of LST observations as input in a data assimilation scheme able to retrieve optimal surface states and parameters that describe energy balance at the land surface. Satellite data from SEVIRI sensor aboard the Meteosat Second Generation (MSG) are used as LST input. A parsimonious 1-D multiscale variational assimilation method has been followed, based on a simplified description of the LST dynamics, the Force-Restore Equation (Lin, 1980; Dickinson, 1988), used as physical constraint. A simplified surface energy budget model (Caparrini, 2001; Caparrini et al., 2004), ACHAB, that includes this assimilation scheme, has been coupled in this study with a limited area atmospheric model, RAMS (Tremback, 1990), in order to study the effects on the latter in terms either of reconstruction of the ground conditions and of vertical characterization of the lower atmosphere. The representation of the land surface processes in RAMS became more and more complex in last years (Lu et al., 2001; Adegoke et al., 2003; Cotton et al., 2003; Walko and Tremback, 2005). Several diagnostics have been performed in order to compare the performances of the runs of RAMS with the ACHAB-RAMS coupling. Particular attention has been devoted to the analysis of the precipitation and local recycling ratio maps have been computed. In the following sections the ACHAB and RAMS models will be described, then the results of the coupling experiment will be exposed. The study has been focused on the Tuscany region, on a domain of about 40 000 km<sup>2</sup> in central Italy, in a period of 4 months, from June to September 2005.

## 2 Surface energy budget model ACHAB

### 2.1 Land surface energy budget

The estimation of heat fluxes that characterize the energy budget at the surface can be formulated with an inverse approach, given a sequence of land surface temperature observations. In order to retrieve these estimates, the dual-source (DS) version of the model ACHAB (Assimilation Code for Hydrologic-Atmospheric Budget) has been utilized (Caparrini et al., 2004).

The DS formulation largely follows Kustas et al. (1996), that describes the soil-vegetation system as a resistance network that includes nodes at the soil, the canopy leaves, the within canopy air and air above the canopy. The conductances are characterized through turbulent heat transfer coefficients  $C_{Hs}$  (for heat transfer from soil to air within the canopy) and  $C_{Hv}$  (from leaves to air within the canopy). Following the bulk parametrization, the sensible heat fluxes (soil and vegetation respectively) are given by:

$$H_s = \rho c_p C_{Hs} U_{ca} (T_s - T_{ca}) ; \quad (1a)$$

$$H_v = \rho c_p C_{Hv} U_{ca} (T_v - T_{ca}) \quad (1b)$$

where  $\rho$  is the air density,  $c_p$  is the specific heat of the air at constant pressure,  $T_s$  and  $T_v$  are respectively soil and canopy kinetic temperatures, and  $T_{ca}$  and  $U_{ca}$  are the temperature of the air and the wind speed at a reference height within the canopy volume.

The turbulent moisture flux is represented using the definition of evaporative fraction EF for soil and vegetation:

$$EF_s = \frac{LE_s}{LE_s + H_s} ; \quad (2a)$$

$$EF_v = \frac{LE_v}{LE_v + H_v} \quad (2b)$$

where  $L$  is the specific latent heat of vaporization and  $E_s$  and  $E_v$  are the moisture fluxes in mass per unit of contributing surface (soil and vegetation, respectively).

The total heat fluxes  $H$  and  $LE$  can be calculated by means of a bulk heat transfer coefficient  $C_H$  from the air within the canopy to the boundary layer air above the canopy (subscript  $a$ ):

$$H = \rho c_p C_H U (T_{ca} - T_a) \quad (3)$$

where  $U$  is the wind speed above the canopy. In analogy to Eq. (2a–b), the total evaporative flux  $LE$  is determined by means of the total evaporative fraction  $EF$ . The total sensible and latent fluxes for a pixel are given by the contribution of the fluxes from the soil and the vegetation components, weighted by the fractional vegetation cover  $f$ .

The assimilation procedure comprehends an adjoint model constituted by the Force-Restore equation (Lin, 1980; Dickinson, 1988). The Force-Restore equation is a simplified description of the dynamic of the LST in which are present a

forcing term (first on the right side, given by the energy budget at the surface) and a restoring term (second on the right side, that takes into account the effect of the deep ground temperature  $T_{\text{deep}}$ ):

$$\frac{dT_s}{dt} = 2\sqrt{\pi\omega} \frac{R_n - H - \text{LE}}{P} - 2\pi\omega (T_s - T_{\text{deep}}) \quad (4)$$

where  $H$  and  $\text{LE}$  are positive upward,  $R_n$  is net surface radiation, positive downward,  $P$  is thermal inertia [ $\text{J}/(\text{m}^2 \cdot \text{K} \cdot \text{s}^{1/2})$ ] and it is assumed that the forcing has a dominant frequency  $\omega$  (i.e. diurnal). Moreover, in land surface models it is often assumed that the energy balance in the canopy is an instantaneous (no inertia) balance between net radiation and turbulent fluxes ( $R_n = H_v + \text{LE}_v$ ), due to the fact that the vegetation canopy has a much lower thermal inertia compared to soil. Written in terms of EF, the canopy energy balance model now becomes:

$$R_n = \frac{H_v}{1 - \text{EF}_v} \quad (5)$$

The relations (4) and (5) constitute the energy budget constraint of the problem, respectively for soil and vegetation. The DS model consists of the set of equations of turbulent fluxes (Eqs. 1a–b, 2a–b, and 3) and of constraints on the energy budgets (Eqs. 4 and 5) with parameters  $C_{H_s}$ ,  $C_{H_v}$ ,  $C_H$ ,  $\text{EF}_s$ , and  $\text{EF}_v$  that need to be estimated. Following Eagleson (2002), the conductances of vegetation and soil layers can be estimated as a function of the air heat transfer coefficient  $C_H$  and the measured wind speed  $U$ . The unknown parameters to be estimated are so reduced to  $C_H$ ,  $\text{EF}_v$ , and  $\text{EF}_s$ .

## 2.2 Assimilation of LST into ACHAB

The assimilation process consists in the minimization of a cost functional  $J$  that incorporates physical constraints (energy balance) through Lagrange multipliers. The functional  $J$  contains a quadratic measure of the misfit between model predictions and LST observations. The minimization is carried on under the working hypotheses of constant evaporative fractions during daytime hours (Sugita and Brutsaert, 1991; Crago and Brutsaert, 1996) and constant neutral heat transfer coefficient  $C_{\text{HN}}$  (related to  $C_H$  through a coefficient for the atmospheric stability correction) over a longer timescale (e.g., a month).

The functional is constructed using two different integral time scales: the overall assimilation period of length  $D$  days, for which a single  $C_{\text{HN}}$  value is estimated at each state pixel; a daily assimilation window  $[t_0, t_1]$  during which EF may be considered constant and  $\text{EF}_s$  and  $\text{EF}_v$  are estimated for each pixel independently for each day  $d=1, \dots, D$ . The scalar cost function  $J$  is:

$$J = \sum_{d=1}^D \sum_{k:t_k \in [t_0, t_1]} [\overline{T_{\text{obs},k}} - \mathbf{M} \cdot \overline{\mathbf{T}_R}(t_k)]^T$$

$$\begin{aligned} & \mathbf{G}_{\mathbf{T}_s}^{-1} [\overline{T_{\text{obs}}}, k - \mathbf{M} \cdot \overline{\mathbf{T}_R}(t_k)] + \\ & + \sum_{d=1}^D [\overline{\mathbf{EF}_{s,d}} - \overline{\mathbf{EF}'_{s,d}}]^T \mathbf{G}_{\mathbf{EF}_s}^{-1} [\overline{\mathbf{EF}_{s,d}} - \overline{\mathbf{EF}'_{s,d}}] + \\ & + \sum_{d=1}^D [\overline{\mathbf{EF}_{v,d}} - \overline{\mathbf{EF}'_{v,d}}]^T \mathbf{G}_{\mathbf{EF}_v}^{-1} [\overline{\mathbf{EF}_{v,d}} - \overline{\mathbf{EF}'_{v,d}}] + \\ & + [\overline{\mathbf{C}_{\text{HN}}} - \overline{\mathbf{C}'_{\text{HN}}}]^T \mathbf{G}_{\mathbf{C}_{\text{HN}}} [\overline{\mathbf{C}_{\text{HN}}} - \overline{\mathbf{C}'_{\text{HN}}}] + \\ & + \sum_{d=1}^D \int_{t \in [t_0, t_1]_d} \overline{\Lambda}^T \left[ \frac{dT_s}{dt} - F(\overline{T_s}, \overline{\mathbf{EF}_{s,d}}, \overline{\mathbf{EF}_{v,d}}, \overline{\mathbf{C}_{\text{HN}}}) \right] dt \quad (6) \end{aligned}$$

in which the first term is the quadratic measure of the misfit between model predictions and LST observations, is the vector of  $n$  model states at time  $t$ , are the observations at irregular times  $t_k$ .  $\mathbf{M}$  is a matrix of measurements-to-model LST projection factors,  $D$  is the number of days considered,  $[t_0, t_1]$  is the assimilation window,  $\overline{\Lambda}$  is the vector of Lagrange multipliers,  $\mathbf{G}_{\mathbf{T}_s}$ ,  $\mathbf{G}_{\mathbf{EF}_s}$ ,  $\mathbf{G}_{\mathbf{EF}_v}$ , and  $\mathbf{G}_{\mathbf{C}_{\text{HN}}}$  are the spatial covariance matrices for observations and parameters (in this application assumed as diagonal), the primed variables represent prior estimates of parameter values and the last term represents the physical constraint. The correct values for the parameters  $C_{\text{HN}}$  and EF can be found minimizing  $J$ , thus imposing the vanishing of its first variation ( $\delta J=0$ ).

The model solves the Euler-Lagrange equations (that come from imposing the conditions  $J=0$ ) through an iterative procedure on monthly basis. The model has been run, for each day of the period of interest, inside the temporal window 6 a.m.–6 p.m. at half an hour timestep. ACHAB requires as input, together with the LST observations at an half-an-hour timestep during the assimilation temporal window, standard micrometeorological measurements: air temperature, air humidity, wind speed and incoming solar radiation. A LAI map is also used to characterize the fractional vegetation cover. The assimilation procedure has been carried on only on the domain cells for which a sufficient number of LST observations (at least three values per day) and meteorological forcing was present. In the cells where these requirements were not satisfied (cloudy cells), a forward integration (without assimilation) of the Force-Restore equation has been performed, in order to assure proper forcing for RAMS on the whole domain.

The estimated parameters maps have been produced on a monthly basis for  $C_H$  and on daily basis for both  $\text{EF}_s$ ,  $\text{EF}_v$ . Together with parameters, maps for each timestep (inside the diurnal assimilation window) have been produced for the following variables: sensible and latent heat flux from soil component  $H_s$ ,  $Le_s$  and from vegetation component  $H_v$ ,  $Le_v$ , soil, vegetation and canopy air temperatures  $T_s$ ,  $T_v$ ,  $T_{ca}$ , and mixing ratio  $r_s$ ,  $r_v$ ,  $r_{ca}$ .

### 3 Atmospheric model RAMS

The Regional Atmospheric Modelling System (RAMS) is a limited area atmospheric model with complete physics and non-hydrostatic equations, developed at the Colorado State University. It solves a set of equations that describe dynamics and thermodynamics of the atmosphere, mass and energy conservation and hydrometeors microphysics (Tremback, 1990). RAMS presents a number of different numerical scheme for convection, radiation, cloud microphysics and boundary conditions. The model is able to work on nested grids configurations, allowing to simulate the area of interest at very high spatial resolution without losing the information from medium or synoptic scale atmospheric features. It also provides a nudging scheme that allows the assimilation of measures inside the boundary conditions, that are required on a 6-h basis. The scheme is able to assimilate ground point measures and atmospheric soundings by merging them with the boundary conditions. In the present study the model has been used in non-hydrostatic configuration and a set of calibration runs based on ground measurements and on literature on RAMS and its use in the Mediterranean area (Tremback, 1990; Meneguzzo et al., 2002; Gualtieri and Calastrini, 2003; Pasqui et al., 2004) has been performed in order to retrieve the best possible configuration of the model for the domain of study.

RAMS comprehends the surface-atmosphere interaction scheme LEAF-3 (Land Ecosystem-Atmosphere Feedback version 3; Walko and Tremback, 2005). LEAF-3 utilizes a detailed modelling of the interactions between the atmosphere, the soil, the vegetation, the surface water and the deep ground, taking into account the characterization of the land cover and of the health status of the vegetation. The main purpose of this module is to compute the heat and humidity exchanges with the atmosphere, providing the lower boundary conditions for the atmosphere in RAMS.

LEAF-3 works on a two-dimensional grid that represents the surface (comprehending soil surface, vegetation, canopy air and, if present, water) and on a three-dimensional grid that covers a thin layer of soil (usually 0.5–1 m thick), subdivided in a customizable number of levels. All components are described with prognostic equations that include exchanges terms such as turbulent fluxes, heat conduction, water diffusion and percolation, longwave and shortwave radiative transfer, transpiration and precipitation.

Figure 1 provides a general scheme of all the components considered in LEAF-3 for a single cell and highlights the energy fluxes exchanged between different components. The interface between the surface and the atmosphere is constituted by a scheme similar to the one employed by ACHAB (see Sect. 2) in which several fluxes (from soil/vegetation to canopy air and from canopy air to atmosphere) are present. The surface fluxes of heat, momentum, and water vapour into the atmosphere are computed with the scheme of Louis (1979). For the three possible types of patch

(water, bare soil, vegetated soil), different temperature and water mass budget are computed.

Even though the turbulent closure considered in both ACHAB and LEAF-3 models is of the first order (bulk formulation), the models are quite different. In particular LEAF-3 is much more detailed (especially relatively to the vegetation component) and requires many more parameters. However, as it will be exposed in Sect. 5, LEAF-3 tends to produce temperature and humidity states and a partitioning of the turbulent fluxes at the surface very different from the typical observed values.

### 4 Case study

Accordingly to the availability of LST satellite observations and micrometeorological data from ground sensors, the domain of study was selected as the Tuscany region in central Italy in 2005. The region, that covers an area of about 23 000 km<sup>2</sup>, is crossed by the Apennines Mountain range that describes an arc from North to East having average elevation of 1000 m a.s.l. with maximum of about 2000 m. The mean annual precipitation is 800 mm, the climatic type can be considered as semi-arid with a high variability during the year; summer is hot and dry while winter is cold and rainy.

The period chosen for the analysis was summer 2005 for a total of four months, from 1 June to 30 September. The choice of the summer period is mainly dictated from the fact that this is the year season in which the land-atmosphere interactions are dominated by heat fluxes from the surface. The summer of 2005 in central Mediterranean was characterized by some short heat wave in the first half (especially during the month of June) followed by a less warm period caused by cold air masses from northern Europe. During this period the precipitation regime was characterized by a number of intense rainfall events of short duration along all the summer and two-three long-duration rainfall periods (from some days to almost a week long). In Fig. 2 the topography of Tuscany and the grids used for the RAMS run are shown: the domain of the study is constituted by the nested grid, that covers most part of the Tuscany (highlighted in the right panel of the figure) and coincide with the ACHAB domain. The reanalysis products from the National Centers of Environmental Prediction (NCEP) of the US National Weather Service have been used for lateral boundary conditions.

The main input of the assimilation procedure are the estimates of Land Surface Temperature, obtained from the Meteosat Second Generation SEVIRI sensor by the Land Satellite Application Facility (Land SAF Project Team, 2006). The micrometeorological input data (solar radiation, air temperature, air humidity, wind speed) have been obtained from the ground-based networks of Tuscany Region Hydrological Service.

The ACHAB model has been run on four separate monthly runs (June, July, August, and September 2005) in order to

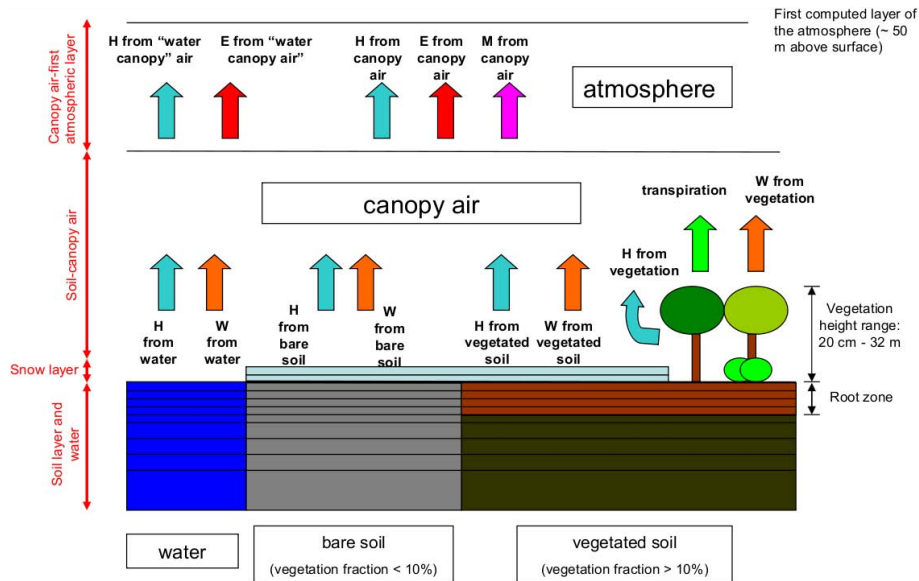


**Fig. 1.** General scheme of energy exchanges inside a single cell in LEAF-3. Fluxes between main components are indicated with  $H$  (sensible heat flux),  $E$  (latent heat flux) and  $M$  (momentum flux).

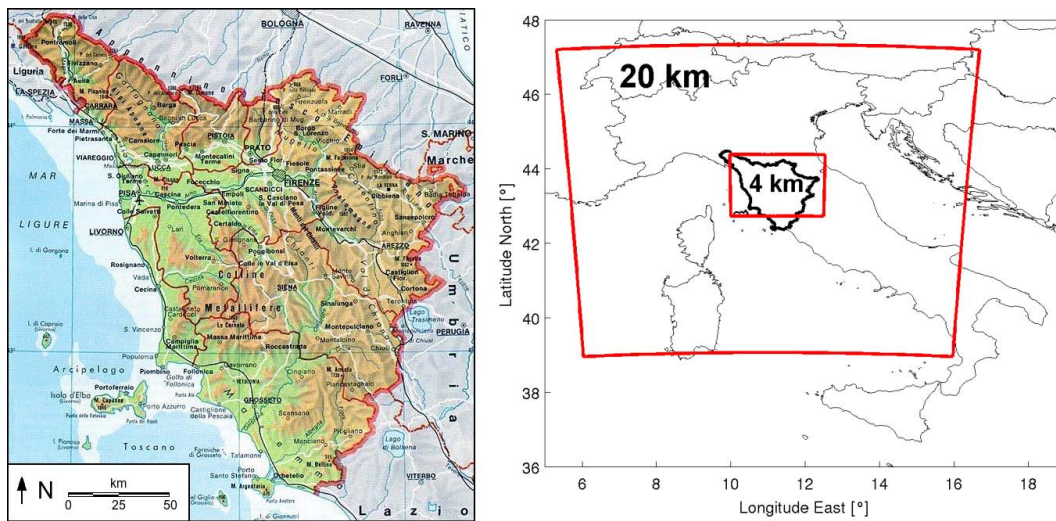


**Fig. 2.** Topography of Tuscany (left panel) and nested grids configuration with spatial resolutions in RAMS model (right panel). The nested grid at 4 km of horizontal resolution centred on Tuscany (highlighted in the right panel) constitutes the domain of the study.

allow a monthly estimate of the parameter  $C_H$ , while evaporative fraction maps for both soil and vegetation components have been produced for each day.

### 5 Coupling of the models and results

This section describes the coupling between ACHAB and RAMS and the results of this numerical experiment. The purpose of this coupling was to explore the land-surface interactions inside the atmospheric model forced by the results of the LST assimilation with ACHAB.

The coupling has been realized replacing the estimates of sensible and latent heat fluxes and of temperature and humidity states at the surface produced by ACHAB inside the surface module of RAMS, LEAF-3 (see Sect. 3). The atmospheric model has been modified in order to acquire, during the atmospheric simulation and inside the diurnal window of each day, the maps of all the variables estimated by ACHAB and bypass the computations of LEAF-3. In analogous works land data were directly assimilated inside the atmospheric model (McNider et al., 1994; Giard and Bazile, 2000; Mahfouf et al., 2000; Bélair et al., 2003a, b) or surface states like

the soil moisture were modified in order to match the observations of related variables (Jones et al., 1998a, b). Differently from these studies, in the present work a replacement of the surface states has been performed using the products of a separated land-surface model.

Several diagnostic tests have been executed on all the results of the experiment, in order to evaluate the effects of the coupling on the near-surface variables reconstruction. The influence on vertical profiles of the atmosphere and on the generation of precipitation events has been also considered.

### 5.1 ACHAB runs results

Besides the parameters  $C_H$ ,  $EF_s$  and  $EF_v$ , that characterize the surface energy budget, the products from ACHAB are constituted by surface energy and water fluxes and surface states in terms of temperature and humidity of the soil and vegetation components. Figure 3 shows the comparison between ACHAB and the control RAMS run (without coupling) in terms of total energy fluxes (soil+vegetation, spatial average). The latent heat fluxes estimated by ACHAB result much higher than the equivalent RAMS variables, while the opposite happens for the sensible heat fluxes. The comparison between the evaporative fractions computed by RAMS and estimated by ACHAB shows how the atmospheric model fails in estimating realistic values of this parameter. RAMS EF are in fact almost always outside the typical observed range 0.5–0.9 (Crago and Brutsaert, 1996), while ACHAB estimates are constantly comprehended between 0.7 and 0.85.

### 5.2 Results of the coupling experiment

The ACHAB products replaced inside LEAF-3 were states of temperature and humidity of soil, vegetation and canopy air and turbulent fluxes of heat and water mass. The replacing has been performed only during the diurnal window 6 a.m.–6 p.m., while during the night the normal functioning of RAMS-LEAF-3 was restored.

Available ground micrometeorological data were also used to validate the results. In Fig. 4 the time series of area-average air temperature at 2 m above the ground for the month of July are compared with temperatures produced in the control run of RAMS and in the coupling experiment. The observed time-series have been obtained by computing the mean of all the stations, while the simulated time-series are computed as the mean of all the nearest gridpoints. The top panel shows how RAMS tended to produce higher temperature with respect to the observations, both during the day and during the night hours. The lower panel shows an improvement of the air temperature in terms of a strong decreasing of the positive bias (that reaches up to 5–6°C at the diurnal peak, see also Table 1) that normally affected the temperature produced by RAMS and that was almost completely eliminated.

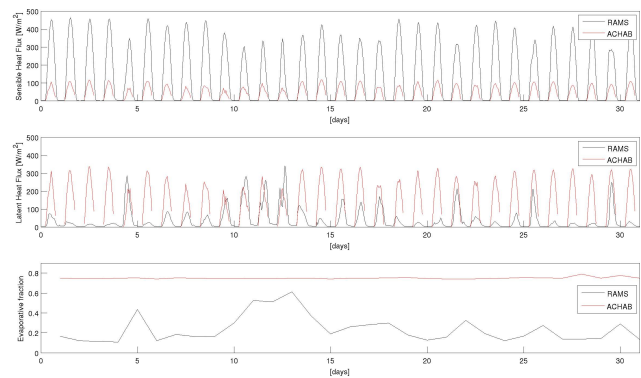


**Fig. 3.** Comparison between total (vegetation+soil) area-averaged sensible heat flux (top panel), latent heat flux (middle panel) and daily evaporative fraction (bottom panel) between RAMS/LEAF-3 (control run) and ACHAB for July 2005.

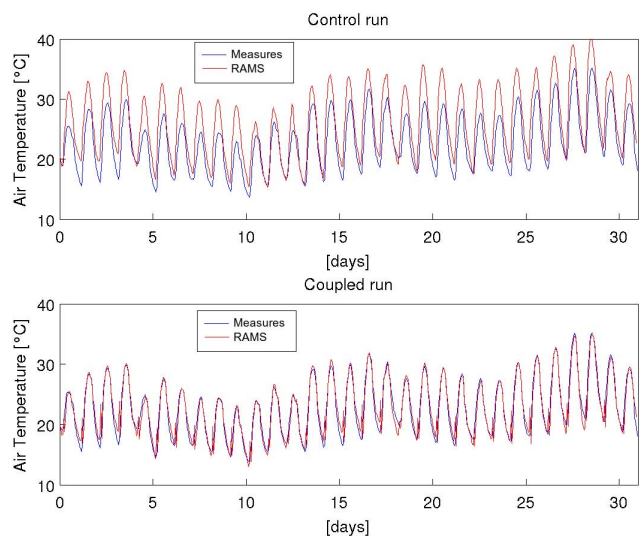


**Fig. 4.** Comparison between observed and simulated average time series of the air temperature at 2 m above the ground for two RAMS runs: control run (top panel) and coupled run (bottom panel). The measures time-series are obtained by computing the mean of all the stations, while the simulated time-series are computed as the mean of all the nearest gridpoints. The period is July 2005.

In Fig. 5 the spatial patterns of the air temperature maps for 2 August are compared. The figure shows the maps produced by the control run (top right) and the coupled run (bottom right) and the observed map obtained through interpolation of the ground measurements (left). The maps show that changes in spatial patterns occurred due to the assimilation procedure. In particular, differences in the pattern of the plain region of the map are evident, while the mountainous regions (the Apennines, in the northern part) present a similar spatial distribution of the temperature. With regard to the comparison with the observations, the best accord in terms of temperature of the mountainous regions is given by the control run, while the coupled run provided better results on the

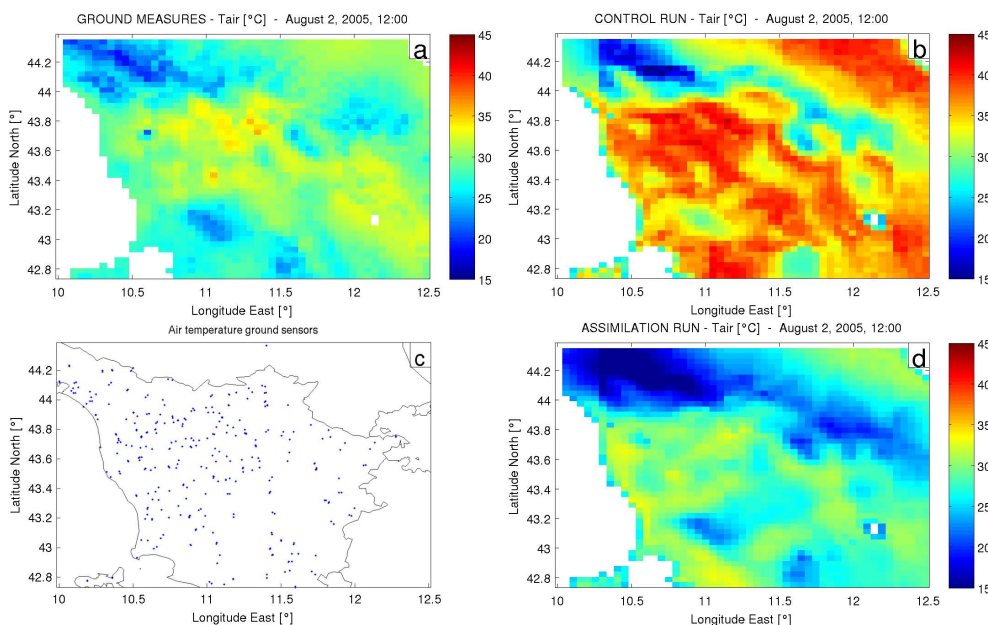


**Fig. 5.** Comparison between the air temperature maps for 2 August 2005 at midday. On the top-left panel the map obtained from interpolation of the ground thermometers is shown. On the right, the maps produced by the control run (top-right) and the coupled run (bottom-right) are present. In the bottom-left panel the location of the ground temperature sensors is present.

**Table 1.** Comparison between the two atmospheric runs in terms of reconstruction of the temperature and humidity of the air at 2 m above the ground. RMSE and BIAS with respect to the measured time series for the whole period are shown.

Run	Surface variables comparison			
	Air temperature	Air relative humidity	Air temperature	Air relative humidity
	RMSE	RMSE	BIAS	BIAS
	[°C]	[%]	[°C]	[%]
Control run	3.53	21.01	3.18	-16.53
Coupled run	1.81	9.9	-0.01	0.77

plain part of the domain, underestimating the temperatures at higher heights. However, different patterns are observed in the plain regions between the observations and the coupled run. Both the control and the coupled runs present a decreasing of the temperature along the coastal line.

A significant improvement was reached also in terms of air humidity: in Fig. 6, the time series of the air relative humidity at 2 m above the ground is compared with the equivalent product of RAMS in control and coupled runs. Again, the time-series are obtained by computing the mean of all the stations for the observations and of all the nearest grid-points for the simulation. The humidity produced by the control run shows a strong underestimation during most part of the month, especially during the night. In the period comprehended between days from 10 to 18, on the opposite, the

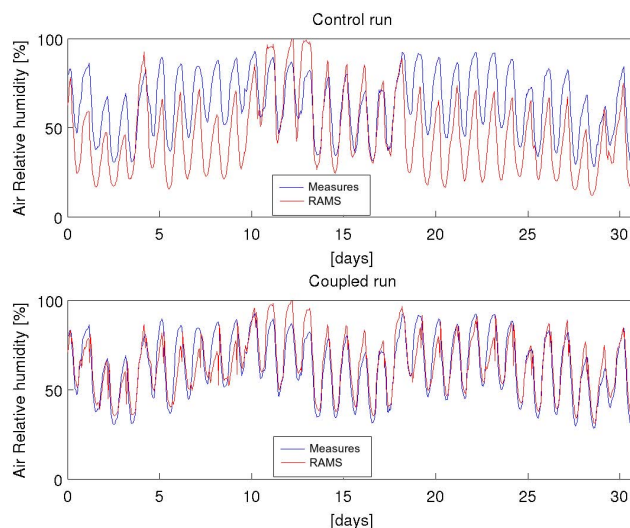


**Fig. 6.** Comparison between the observed and simulated average time series of the air relative humidity at 2 m above the ground for two RAMS run: control run (top panel) and coupled run (bottom panel). The measures time-series are obtained by computing the mean of all the stations, while the simulated time-series are computed as the mean of all the nearest gridpoints. The period is July 2005.

humidity is overestimated during the day, in correspondence with rainy days. The coupling experiment mostly corrected such underestimation, during both diurnal and nocturnal periods. In particular, a slight nocturnal overestimation was introduced.

Figure 7, analogously with Fig. 5, shows the comparison between air humidity maps, expressed in terms of air mixing ratio at the surface. In this case it is evident how the control atmospheric simulation fails in reconstructing the correct spatial pattern at the surface. RAMS produced, in fact, an almost constant distribution of humidity, apart the coastal regions where an abrupt increasing is evident. On the opposite, the coupled run shows improvement in terms either of values range and of spatial distribution, showing a central part of the map with lower humidity and higher values on the East and on the western coast. With respect to the observations map it can be noticed a slight underestimation of the mixing ratio in correspondence of the coasts and an overestimation of similar extent of the inland part of the domain.

The comparison between the runs in terms of spatially-averaged cumulated precipitation in the whole four months long period is presented in Fig. 8. In the control run and in the coupling experiment the precipitation periods result essentially the same; no significant changes either in temporal distribution and in total precipitated volume are observed. This can be explained with the dominant role of the lateral boundary conditions, that have not been modified by the coupling, in providing the availability of atmospheric moisture. In both simulations RAMS generated more precipitation events, while the coupling procedure led to a slightly smaller quantity of total precipitation.

In Fig. 9 the cumulated daily precipitation maps for 7 July are represented. While the cumulated curves (Fig. 8) do not show significant differences between the runs, both simulations produced spatial patterns very different from the observations. In the panel (a) (observed rainfall), the most part of the precipitation is concentrated on the west coast of the domain. On the opposite, both atmospheric simulations generated sparse low-intensity rainfall on the whole domain with higher rainfall height in the north-eastern region in the control run (panel b) and some minor events in the coupled run (panel d).

The different behaviour in space and time of the precipitation can be explained considering the different effects of the lateral and the lower boundary conditions. Being the size of the nested grid relatively small (about 40 000 km<sup>2</sup>), the moisture circulation of the domain is largely determined by the lateral boundary conditions, that impose the humidity advection (Seth and Giorgi, 1998). On the other side, the convection is affected by the lower bound forcing that, by means of the coupling with ACHAB, is completely replaced during the diurnal period. The combination of these two effects creates a situation in which the availability of atmospheric water is determined from without the domain, while the conditions that can trigger the precipitation depend on the surface fluxes forcing (temperature and humidity at the surface, evapotranspiration fluxes, see for example Eltahir and Pal, 1996; Fabry, 2006; Yuang et al., 2007). The coupling of the models, in this case, can affect only partially the dynamics of the atmospheric domain, but shows that also in such a

constrained situation a significant influence is observed (see also Sect. 5.3).

The Tables 1 and 2 resume the results of the control run and the coupling experiment in terms of comparison between observations and atmospheric simulations. From Table 1 the RMSE of the surface states (air temperature and humidity) has been halved following the coupling with ACHAB. For both variables, the bias was almost eliminated. Table 2 shows how the model overestimated the monthly total precipitation in June and September and underestimated the same variable in July and August.

As stated in Sect. 3, when ground measures or atmospheric soundings are available, it is possible to make RAMS assimilate these data inside its boundary conditions with a nudging procedure. A number of runs in which RAMS assimilated measures from the available ground sensors have been performed. The results showed that, despite the large quantity of measures available, there have been no significant effects on the atmospheric simulation, confirming the added value given by the satellite estimations of LST.

An important variable for the characterization of the lower atmosphere is the height of the planetary boundary layer. For the latitudes of the domain of this study the PBL height varies from some tens of meters during nocturnal period up to 1.5–2 km at the midday peak in a sunny day (Stull, 1988). The PBL height computed in the control run of RAMS showed unrealistic high values, reaching a maximum of 4 km above the surface, while the mean values of the diurnal peaks is about 2.5 km. The coupled run produced much lower PBL peaks with mean height equal to about 1–1.5 km, much more similar to the expected values for a mid-latitude region.

As a further characterization of the precipitation, a *recycling ratio* analysis was carried on. As stated in Sect. 1, the feedback processes in terms of water exchanges between the soil and the atmosphere are of major importance for the climate studies. A possible characterization of these feedbacks is given by the precipitation recycling, that is a measure of how much evaporation in a continental region contributes to the precipitation in the same region. It is commonly characterized by the recycling ratio, that expresses the fraction of local-originated precipitation to the total precipitation in the considered domain (Burde and Zangvil, 2001).

In this work the recycling model of Eltahir and Bras (1994) has been employed. This model allows the computation of maps of the *local* recycling ratio  $\rho$ , defined, for a small area  $\Delta A$ , as the fraction of precipitation originated from evaporation from the whole domain of area  $A$  on the total precipitation that falls on  $\Delta A$ . With this model, maps of  $\rho$  and estimates of the recycling ratio  $r$  have been computed on a monthly basis. In Fig. 10 the comparison between  $\rho$  maps for July in control run and coupled run is shown, while in Table 3 the monthly values of the recycling ratio for the whole period are reported.

The recycling ratio time series showed a net increasing in the coupling experiment. Following the replacing of the sur-

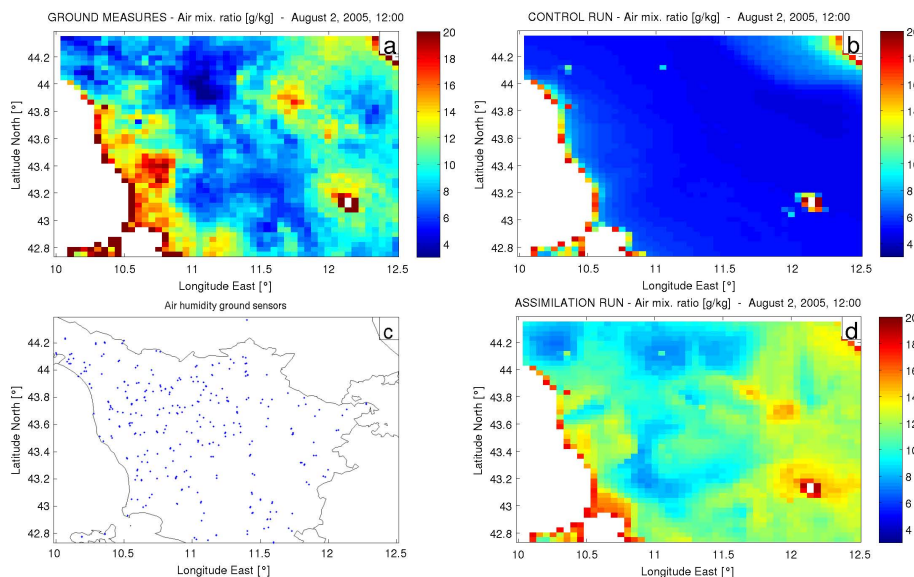


**Fig. 7.** Comparison between the air humidity maps expressed as mixing ratio for 2 August 2005 at midday. On the top-left panel the map obtained from interpolation of the ground sensors is shown. On the right, the maps produced by the control run (top-right panel) and the coupled run (bottom-right panel) are present. In the bottom-left panel the location of the ground sensors is present.

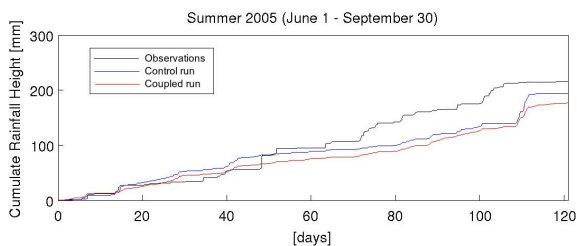


**Fig. 8.** Comparison of the cumulated rainfall height for summer 2005. Time series of the measures (black line), of the results of the control RAMS run (blue) and of the coupling experiment (red) are shown. The whole domain has been considered.

**Table 2.** Monthly cumulated rainfall height for control run and for coupling experiment. The whole domain has been considered.

Run	Cumulated rainfall height [mm]				
	June	July	August	September	Total
Observations	33.8	61.1	69.7	51.4	216
Control run	52.5	36.7	31.8	73.4	194.4
Coupled run	45.2	30.8	37.4	63.1	176.5

**Table 3.** Monthly-averaged recycling ratio for the whole period for control run and for coupling experiment. The whole domain has been considered.

Run	Monthly-averaged Recycling ratio [%]			
	June	July	August	September
Control run	7.2	2.6	3.9	7.5
Coupled run	17.1	7.6	12.5	14.1

face energy budget, the coupling with ACHAB resulted in an increase of the relative importance of evaporation fluxes in the economy of the precipitation. The result is confirmed by the fact that the total rainfall volumes were substantially unchanged (see Fig. 8 and Table 2), while the latent heat fluxes considerably increased (Fig. 3). The recycling ratio maps show also a change in spatial patterns: while both maps show an increasing of  $\rho$  eastward, the coupled run produces a different spatial distribution. Due to the fact that the information necessary to produce these maps comes from evaporation and wind fields, the different  $\rho$  maps show how the introduction of different lower boundary conditions led to a change in the atmospheric circulation in the domain.

## 6 Conclusions

The different components of the energy balance at the land surface are recognized as fundamental quantities in many hydrological and meteorological problems. In particular, it is largely argued that surface evaporation fluxes may have strong influences on the atmospheric processes that lead to precipitation, as a mean of feedback from soil-moisture. From this point of view the remote sensing technologies

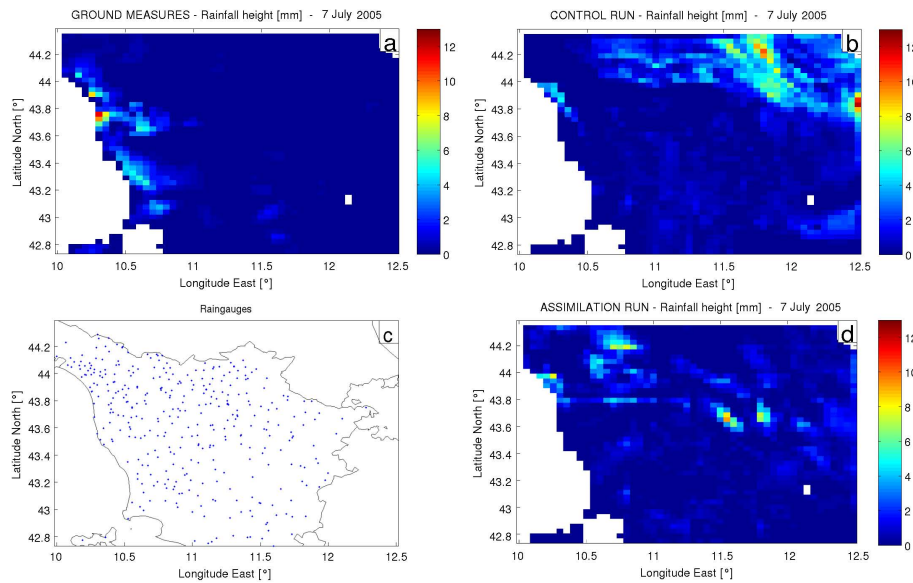


**Fig. 9.** Maps of daily cumulated precipitation (in mm) for 7 July 2005. On the top-left panel the map obtained for interpolation of the ground rain gauges is shown. On the right, the maps produced by the control run (top-right panel) and the coupled run (bottom-right panel) are present. In the bottom-left panel the location of the rain gauges is present.

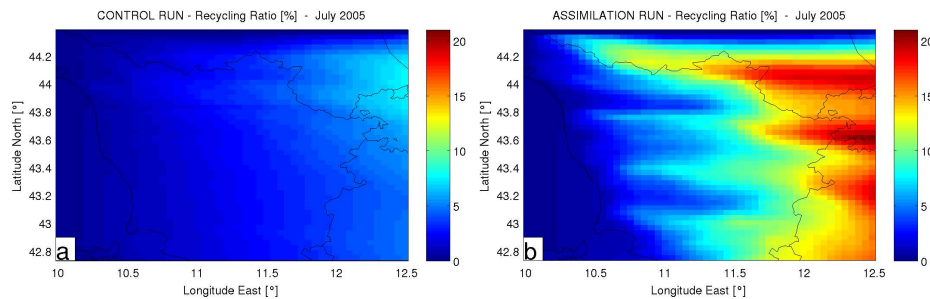


**Fig. 10.** Maps of the local recycling ratio for control run (left) and coupling experiment (right) for July 2005.

allow to map a number of surface-related characteristics on large areas. Consolidated data assimilation techniques, like the one utilized in this research, allow to retrieve variables of interest that can characterize these surface phenomena by merging data and theoretical models.

The present study introduced a coupling framework in which the ACHAB model, that assimilate remotely sensed maps of LST in order to characterize the surface energy budget, and RAMS, a non hydrostatic limited area atmospheric model, interact. The land-surface interactions inside this two-models setup has been analysed with special focus on different lower boundary conditions.

The results showed that the substitution of the surface energy budget changed significantly the behaviour of the atmospheric model, particularly at the ground surface. The coupling led to improvements in RAMS performances in terms of reconstructing surface variables such as air temperature and humidity. In particular, strong biases present in the at-

mospheric control simulations have been almost completely eliminated, while the computed RMSE has been reduced of about 50% following the coupling. Different spatial patterns of these near-surface variables have been obtained, with remarkable improvements for what concern the air humidity at 2 m above the ground. The accurate reconstruction of the surface energy fluxes, which enter as lower boundary conditions for the atmospheric model, brought improvements in the vertical characterization of the atmosphere.

Significant changes in the spatial patterns of the precipitation have been also observed after including the data assimilation, even though the temporal distribution of the rainfall events was substantially unchanged. This result was confirmed by the estimated global and local recycling ratio, that showed noticeable increasing and change in spatial pattern when coupling was introduced.

As further result of the work, the coupling procedure can also be viewed as an assimilation framework that allows

the atmospheric model to assimilate measurements of surface variables, both from ground stations and satellite. This procedure is nominally available in RAMS, but experiments done in this study showed that it does not produce significant effects on the results of the simulation.

In conclusions, the study showed the performances of a coupling framework between a surface budget model that assimilates LST and an atmospheric model. Previous works described coupling experiments between atmospheric and surface energy budget models were carried out (Dudhia and Chen, 1999; Haggag et al., 2008). With respect to them, the present study introduces the replacement of the surface module of the atmospheric model with a simplified scheme that includes an high resolution LST assimilation in a complex orography domain. Future researches will focus on the extension of the analysis to larger domains considering also comparison with available atmospheric soundings. The use of complete land-surface scheme will be included into the assimilation framework. Due to the fact that the coupling is possible through quite simple changes to the code of any atmospheric model, it is possible to adapt the procedure to other atmospheric numerical codes. Future studies could be carried out on the possibility to utilize the coupling operationally as a reinitialization procedure for the near-surface variables.

Edited by: S. Michaelides, K. Savvidou, and F. Tymvios

Reviewed by: G. Balsamo and another anonymous referee

## References

- Adegoke, J. O., Pielke, R. A., Eastman, J., Mahmood, R., and Hubbard, K. G.: Impact of Irrigation on Midsummer Surface Fluxes and Temperature under Dry Synoptic Conditions: A Regional Atmospheric Model Study of the U.S. High Plains, *Mon. Weather Rev.*, 131, 556–564, 2003.
- Baldocchi, D.: FLUXNET: A new tool to study the temporal and spatial variability of ecosystem-scale carbon dioxide, water vapor, and energy flux densities, *B. Am. Meteorol. Soc.*, 82, 2415–2434, 2001.
- Bélair, S., Brown, R., Mailhot, J., Bilodeau, B., and Delage, Y.: Operational Implementation of the ISBA land surface scheme in the Canadian regional weather forecast model. Part I: Warm season results, *J. Hydrometeorol.*, 4, 352–370, 2003.
- Bélair, S., Brown, R., Mailhot, J., Bilodeau, B., and Delage, Y.: Operational Implementation of the ISBA land surface scheme in the Canadian regional weather forecast model. Part II: Cold season results, *J. Hydrometeorol.* 4, 371–386, 2003.
- Beljaars, A., Balsamo, G., Betts, A., and Viterbo, P.: Atmosphere/surface interactions in the ECMWF model at high latitudes, in: *Proceedings of ECMWF Seminar on Polar meteorology*, 4–8 September 2006, ECMWF, 153–168, 2007.
- Burde, G. I. and Zangvil, A.: The estimation of regional precipitation recycling. Part I: Review of recycling models, *J. Climate*, 14, 2497–2508, 2001.
- Caparrini, F.: Latent and Sensible Heat Fluxes from Remote Sensing of Land Surface, Ph.D. thesis, Università degli Studi di Padova, Università degli Studi di Firenze, Firenze, 2001.
- Caparrini, F., Castelli, F., and Entekhabi, D.: Variational estimation of soil and vegetation turbulent transfer and heat flux parameters from sequences of multisensor imagery, *Water Resour. Res.*, 40, W12515, doi:10.1029/2004WR003358, 2004.
- Cotton, W. R., Pielke Sr., R. A., Walko, R. L., Liston, G. E., Tremback, C. J., Jiang, H., McAnelly, R. L., Harrington, J. Y., Nicholls, M. E., Carrio, G. G., and McFadden, J. P.: RAMS 2001: Current status and future directions, *Meteorol. Atmos. Phys.*, 82(1–4), 5–29, 2003.
- Crago, R. and Brutsaert, W.: Daytime evaporation and the self preservation of the evaporative fraction and the Bowen ratio, *J. Hydrol.*, 178, 241–255, 1996.
- Dickinson, R. E.: The force-restore model for surface temperatures and its generalizations, *J. Climate*, 1, 1086–1097, 1988.
- Dudhia, J. and Chen, F.: Using a Mesoscale Model Coupled to a Land-Surface Model to Simulate Surface Fluxes at High Resolution, *Proceedings of Ninth ARM Science Team Meeting*, San Antonio, Texas, 22–26 March 1999.
- Eagleson, P. S.: *Ecohydrology: Darwinian Expression of Vegetation Form and Function*, Massachusetts Institute of Technology, Cambridge University Press, New York, Cambridge, MA 02139, USA, 443 pp., 2002.
- Eltahir, E. A. B. and Bras, R. L.: Precipitation recycling in the Amazon basin, *Q. J. Roy. Meteor. Soc.*, 120, 861–880, 1994.
- Eltahir, E. A. B. and Pal, J. S.: Relationship between surface conditions and subsequent rainfall in convective storms, *J. Geophys. Res.*, 101(D21), 26237–26245, 1996.
- Entekhabi, D. and Eagleson, P. S.: Land Surface Hydrology Parameterization for Atmospheric General Circulation models Including Subgrid Scale Spatial Variability, *J. Climate*, 2(8), 816–831, 1989.
- Entekhabi, D.: Recent advances in land-atmosphere interaction research, *Rev. Geophys.*, 33(S1), 995–1004, 1995.
- Entekhabi, D., Rodriguez-Iturbe, I. and Castelli, F.: Mutual interaction of soil moisture state and atmospheric processes, *J. Hydrol.*, 184, 3–17, 1996.
- Fabry, F.: The Spatial Variability of Moisture in the Boundary Layer and Its Effect on Convection Initiation: Project-Long Characterization, *Mon. Weather Rev.*, 134, 79–91, 2006.
- Garratt, J. R.: *The Atmospheric Boundary Layer*, Cambridge University Press, Cambridge UK, 1992.
- Giard, D. and Bazile, E.: Implementation of a new assimilation scheme for soil and surface variables in a global NWP model, *Mon. Weather Rev.*, 128, 997–1015, 2000.
- Gualtieri, G. and Calastrini, F.: A 3-D meteorological archive based on the RAMS model daily forecasting, *Proceedings from “ECAM 2003”*, Ufficio Generale di Meteorologia dell’Aeronautica Militare, Rome, 15–19 Settembre 2003.
- Haggag, M., Yamashita, T., Lee, H., and Kim, K.: A coupled atmosphere and multi-layer land surface model for improving heavy rainfall simulation, *Hydrol. Earth Syst. Sci. Discuss.*, 5, 1067–1100, 2008, <http://www.hydrol-earth-syst-sci-discuss.net/5/1067/2008/>.
- Harris, P. P. and Taylor, C. M.: Assimilation of MSG land-surface temperature into land-surface model simulations to constrain estimates of surface energy budget in West Africa, *Second Interna-*

- tional AMMA Conference, Karlsruhe, 26–30 November 2007.
- Jones, A., Guch, I., and Vonder Haar, T.: Data assimilation of satellite-derived heating rates as proxy surface wetness data into a regional atmospheric mesoscale model. Part I: Methodology, *Mon. Weather Rev.*, 126, 634–645, 1998.
- Jones, A., Guch, I., and Vonder Haar, T.: Data assimilation of satellite-derived heating rates as proxy surface wetness data into a regional atmospheric mesoscale model. Part II: A case study, *Mon. Weather Rev.*, 126, 646–667, 1998.
- Juang, J.-Y., Katul, G. G., Porporato, A., Stoy, P. C., Siqueira, M. S., Detto, M., Kim, H. S., and Oren, R.: Eco-hydrological controls on summertime convective rainfall triggers, *Global Change Biol.*, 13, 887–896, 2007.
- Koster, R. D. and Suarez, M. J.: Climate variability studies with a coupled land/atmosphere model, *Proceedings of the Yokohama Symposium, IAHS Publ.*, 214 pp., July 1993.
- Kustas, W. P., Humes, K. S., Norman, J. M., and Moran, S. M.: Single- and dual-source modeling of surface energy fluxes with radiometric surface temperature, *J. Appl. Meteorol.*, 35, 110–121, 1996.
- Land SAF Project Team: Product User Manual LAND SURFACE TEMPERATURE, <http://landsaf.meteo.pt>, 2006.
- Lin, J. D.: On the force-restore methods for prediction of ground surface temperature, *J. Appl. Meteorol.*, 31, 480–484, 1980.
- Louis, J. F.: A parametric model of vertical eddy fluxes in the atmosphere, *Bound.-Lay. Meteorol.*, 17, 187–202, 1979.
- Lu, L., Pielke, R. A., Liston, G. E., Parton, W. J., Ojima, D., and Hartman, M.: Implementation of a Two-Way Interactive Atmospheric and Ecological Model and Its Application to the Central United States, *J. Climate*, 14, 900–919, 2001.
- Mahfouf, J.-F., Viterbo, P., Douville, H., Beljaars, A. C. M., and Saarinen, S.: A revised land-surface analysis scheme in the Integrated Forecasting System, *ECMWF Newsletter*, 88, 8–13, 2000.
- McNider, R., Song, A., Casey, D., Wetzel, P., Crosson, W., and Carlson, T.: Towards a dynamic-thermodynamic assimilation of satellite surface temperature in numerical atmospheric models, *Mon. Weather Rev.*, 122, 2784–2803, 1994.
- Meneguzzo, F., Menduni, G., Maracchi, G., Zipoli, G., Gozzini, B., Grifoni, D., Messeri, G., Pasqui, M., Rossi, M., and Tremback, C. J.: Explicit forecasting of precipitation: sensitivity of model RAMS to surface features, microphysics, convection, resolution, *Mediterranean Storms, 3rd Plinius Conference 2001*, edited by: Deidda, R., Mugnai, A., and Siccardi, F., GNDCI Publ. N. 2560, ISBN 88-8080-031-0, 79–84, 2002.
- Meng, C. L., Li, Z.-L., Zhan, X., Shi, J. C., and Liu, C. Y.: Land surface temperature data assimilation and its impact on evapotranspiration estimates from the Common Land Model, *Water Resour. Res.*, 45, W02421, doi:10.1029/2008WR006971, 2009.
- Pasqui, M., Tremback, C. J., Meneguzzo, F., Giuliani, G., and Gozzini, B.: A soil moisture initialization method, based on antecedent precipitation approach, for regional atmospheric modeling system: a sensitivity study on precipitation and temperature, in: *Proceedings of the 18th Conference on Hydrology, AMS, Seattle*, 2004.
- Schulz, J.-P., Dümenil, L., Polcher, J., Schlosser, C. A., and Xue, Y.: Land surface energy and moisture fluxes: Comparing three models, *J. Appl. Meteorol.*, 37(3), 288–307, 1998.
- Seth, A. and Giorgi F.: The effects of domain choice on summer precipitation: Simulation and sensitivity in a Regional Climate Model, *J. Climate*, 11(10), 2698–2712, 1998.
- Stull, R. N.: *An introduction to Boundary Layer Meteorology*, Kluwer Academic Publisher, Dordrecht, The Netherlands, 1988.
- Sugita, M. and Brutsaert, W.: Daily evaporation over a region from lower boundary layer profiles measured with radiosondes, *Water Resour. Res.*, 27, 747–752, 1991.
- Tremback, C. J.: Numerical simulation of a mesoscale convective complex, model development and numerical results. Ph.D. thesis, Colorado State University Dept. of Atmospheric Science, Fort Collins, CO 80523, Atmos. Sci. Paper No. 465, 1990.
- Van den Hurk, B. J. J. M. and The, H.: Assimilation of satellite derived surface heating rates in a numerical weather prediction model, *KNMI Scientific Rep.*, WR-2002-04, 19 pp., 2002.
- Vidale, P. L. and Stöckli, R.: Prognostic canopy air space solutions for land surface exchanges, *Theor. Appl. Climatol.*, 80(2–4), 245–257, 2005.
- Walko, R. L. and Tremback, C. J.: *ATMET Technical Note 1, Modifications for the Transition from LEAF-2 to LEAF-3, ATMET, LLC, Boulder, Colorado 80308-2195*, <http://www.atmet.com/html/docs/rams/>, 2005.
- Wetzel, P. J., Atlas, D., and Woodward, R. H.: Determining soil moisture from geosynchronous satellite infrared data: a feasibility study, *J. Appl. Meteorol.*, 23, 375–391, 1984.